Application of nondiffracting beams to wireless optical communications

V. Kollárová[a], T. Medřík[a], R. Čelechovský[a], Z. Bouchal[a]
O. Wilfert*[b], Z. Kolka[b]

[a] Faculty of Science, Palacký University, 17. listopadu 50, 772 00 Olomouc
[b]Brno University of Technology, Purkynova 118, Brno, 612 00, Czech Republic

ABSTRACT

In wireless optical communications, information is carried by coherent laser beams propagating through the free space. In realized communication channels, the standard beams created directly in the laser resonator are utilized. In recent time, an increasing attention has been focused on the so-called nondiffracting beams generated by auxiliary optical systems. In this paper, the theoretical and experimental aspects of the nondiffracting propagation of light are discussed and geometrical parameters and physical properties of nondiffracting beams promising for wireless communications reviewed.

Keywords: Bessel beam, wireless communication, optical vortex beam, partially coherent light

1. INTRODUCTION

In wireless optical communications and most of optical applications, the standard laser beams with a transverse intensity distribution given by the Gaussian function are utilized. The intensity spot of the Gaussian beam remains invariant but its size scales during free propagation. As a measure of the beam spreading, the angular divergence is adopted. It is uniquely determined by the ratio of the wavelength and the waist radius of the beam. By means of a decrease of the beam axial intensity, the Rayleigh distance can be introduced. It is unambiguously given by the size of the beam waist and represents the length of the beam propagation region. If the spot size of the Gaussian beam is reduced, the propagation range is necessarily shortened. This restriction is a result of diffraction effects and can be eliminated if the Gaussian beam is transformed to the form of the so-called nondiffracting beam[1,2]. It can be comprehended as an interference field created by plane waves with constant longitudinal component of the wave vector. The situation can be illustrated geometrically by the conical surface created by the wave vectors of the plane waves. If the amplitudes and initial phases of the plane waves are equal, they interfere constructively at the points of the cone axis and an apparent intensity peak appears there. The transverse intensity distribution of the interference field is given by the Bessel function of the first kind and zero-order and remains exactly propagation invariant. The interference field has a beam-like form and resembles a light tube with an infinite length. Such ideal optical field with completely eliminated diffraction is termed nondiffracting beam. In real experimental conditions, only its approximation called pseudo-nondiffracting (P-N) beam is realizable[3]. In this case, the beam intensity depends on the propagation coordinate but inside a propagation region of the well defined length the beam profile remains nearly unchanged.

In the paper, the basic concept, geometrical parameters and experimental realization of the P-N beams are discussed. The particular attention is devoted to physical properties of the P-N beams promising for wireless optical communications. In this connection, a possibility to shape the intensity profile of the P-N beam into a predetermined form[4], to split originally single beam into an array of collinear P-N beams[5,6] and to tune the spatial correlation properties of the P-N beam[7] will be demonstrated. Resistance of the coherent P-N beam against local amplitude and phase perturbations[8] and atmospheric turbulence will be discussed.

2. NONDIFFRACTING PROPAGATION OF LIGHT

2.1 Conception of nondiffracting and pseudo-nondiffracting beams

An ideal monochromatic nondiffracting beam propagating along the z - axis can be described by the complex amplitude U representing a mode-like optical field,

$$U(x,y,z) = u(x,y)\exp(i\omega t - i\beta z), \tag{1}$$

where ω and β are the angular frequency and the propagation constant, respectively. The intensity of the beam $I = |u|^2$ remains unchanged during propagation, and the shape of the beam spot is given by the function u which can be specified applying differential or integral methods. In the differential formalism, the complex amplitude u is sought as a separable solution of the Helmholtz equation[9-11]. The particular attention has been focused on the circular cylindrical and the elliptical cylindrical coordinates for which the transverse amplitude profile u can be expressed by the known functions. In this way, the Bessel and Mathieu beams has been obtained[12]. The more general nondiffracting fields can be effectively examined by means of the integral formalism. In the integral form, the beam profile u can be conveniently expressed applying the circular cylindrical coordinates r and φ as

$$u(r,\varphi) = \frac{ik}{2\pi}\int_0^{2\pi} A(\psi)g(r,\psi)d\psi, \tag{2}$$

where $g(r,\psi) = \exp[i\alpha r\cos(\psi - \varphi)]$ and $A(\psi)$ denotes an arbitrary periodical function. The parameter α can be interpreted by means of the angular spectrum. The angular spectrum G is a function of the angular frequencies ν_x and ν_y and can be obtained as a two-dimensional Fourier transformation of the amplitude u, $G = FT\{u\}$. Applying the radial angular frequency ν defined as $\nu_x = \nu\cos\psi$ and $\nu_y = \nu\sin\psi$, it can be expressed as

$$G(\nu,\psi) = A(\psi)\delta(\nu - \nu_0), \tag{3}$$

where $\nu_0 = \alpha/(2\pi)$. The peculiar properties of the nondiffracting field come from the special composition of its angular spectrum. It contains only single radial angular frequency so that phase differences of the plane wave components remain unchanged under propagation. The nondiffracting field then can be comprehended as an interference field of plane waves whose wave vectors cover a conical surface with the vertex angle $2\theta_0 = 2\arcsin(\lambda\nu_0)$ where λ denotes the wavelength. The amplitudes and phases of the superposed plane waves can be arbitrary. The azimuthal modulation of the angular spectrum $A(\psi)$ provides degrees of freedom utilizable for creation of an infinite number of nondiffracting fields with different intensity profiles.

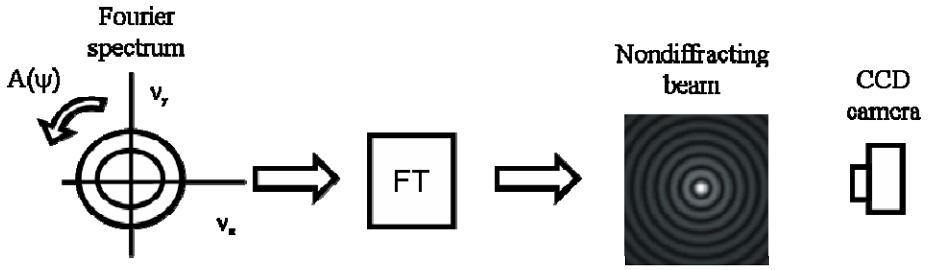

Fig. 1 Shaping of the intensity profile of the nondiffracting beam by an azimuthal modulation of the angular spectrum localized at the Fourier plane.

The azimuthal variability of the angular spectrum of the nondiffracting field is a very strong tool for shaping of the beam intensity profile and can also be used for a splitting of the single beam into an array of the collinear nondiffracting beams. In experiments, the azimuthal modulation can be effectively realized at the Fourier plane of the lens where the angular spectrum of the nondiffracting beam has a form of a thin annular ring (see Fig. 1). By this way, the nondiffracting beams with intensity profiles illustrated in Fig. 2 can be obtained as typical examples.

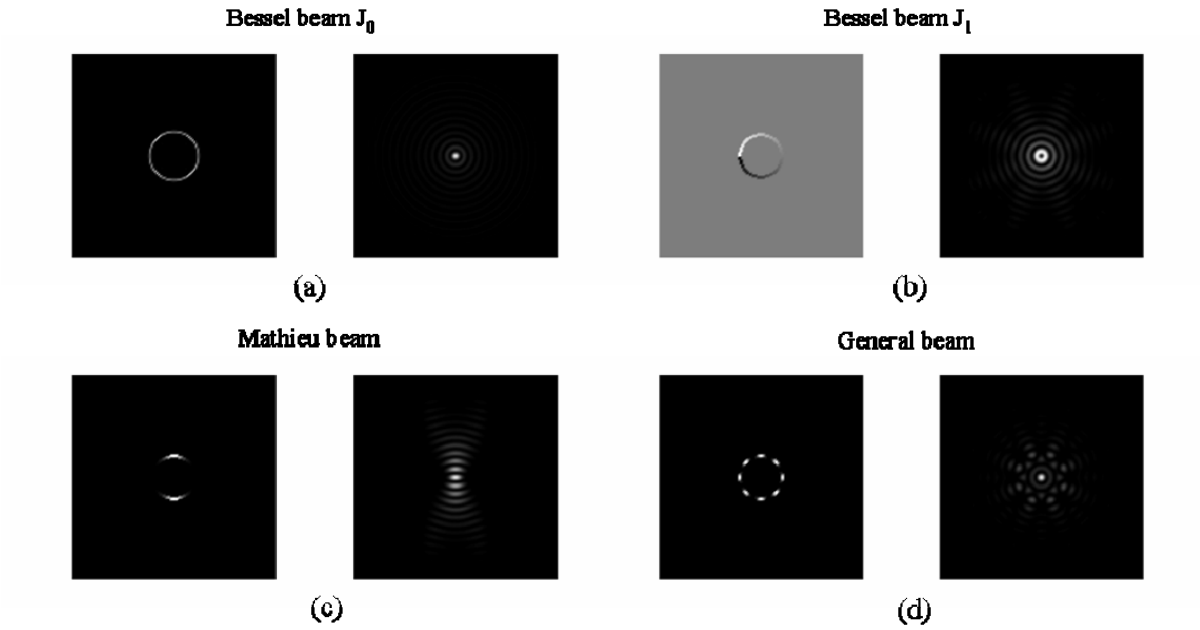

Fig. 2 Intensity profiles of the nondiffracting beams obtained by the azimuthal amplitude and phase modulation of the Fourier spectrum.

In Fig 2 a, the zero-order Bessel beam is illustrated. It has a bright central spot created by interference of plane waves with constant amplitudes and phases so that the spatial spectrum is a ring with a homogeneous intensity. If the phase of the spatial spectrum is modulated by $A = \exp(im\psi)$, the interference of plane results in beam with dark center and the profile is given by the *m*-th order Bessel function. In Fig 2b, the phase of the spatial spectrum and the intensity spot are illustrated for the first-order Bessel beam. Applying the cosine and periodical amplitude modulation of the spatial spectrum, the Mathieu and general beams illustrated in Fig. 2c and 2d are created.

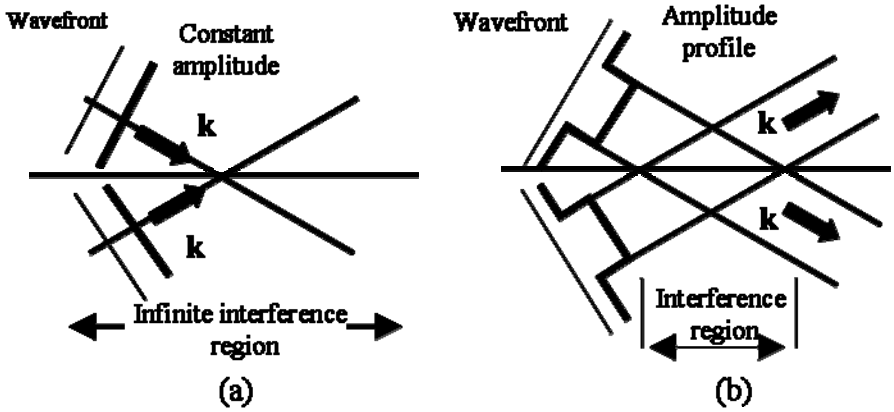

Fig. 3 Interference of the plane waves and the collimated bounded beams resulting in (a) the ideal nondiffracting beam and (b) the pseudo-nondiffracting beam.

The ideal beam-like interference field is created by plane waves of an infinite extent so that the range of beam existence and carried power are also infinite (Fig. 3a). In real conditions, the bounded collimated beams interfere instead of plane waves and the interference region has a finite dimensions depending on the geometry of the experiment. Inside that region, the P-N interference field keeping properties of the nondiffracting beam appears (Fig. 3b).

2.2 Experimental realization of pseudo-nondiffracting beams

As was shown, the ideal nondiffracting beam is an interference field created by the plane waves with the propagation directions restricted by the condition (3). In optics, the required composition of the angular spectrum can be achieved by a spatial filtration at the Fourier plane of the lens. In Fig. 4, the simple optical set-up enabling generation of the P-N beam is illustrated.

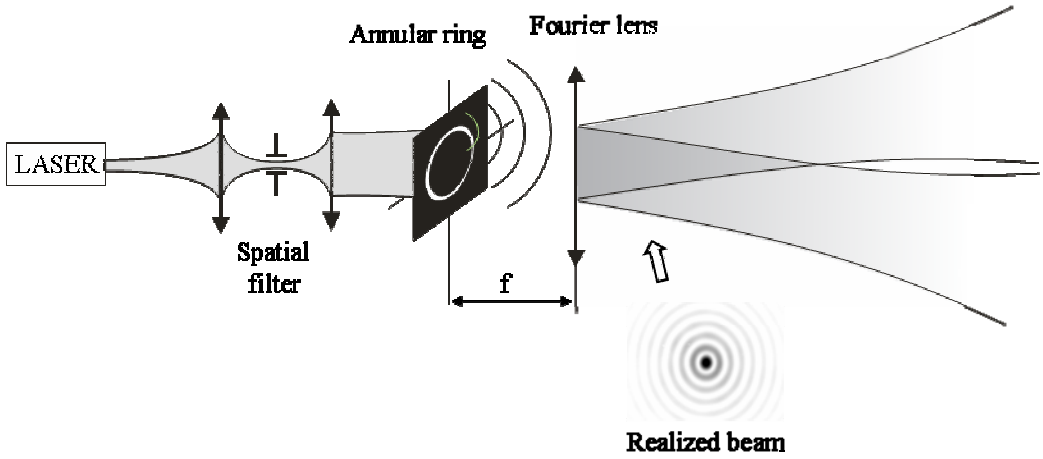

Fig. 4 Generation of the pseudo-nondiffracting beam by means of filtration of the Fourier spatial spectrum.

The thin annular ring placed at the front focal plane of the Fourier lens is illuminated by the spatially filtered and collimated laser beam. Spherical waves rising from each point of the annular ring are transformed by the lens so that the superposition of inclined collimated beams approximating the angular spectrum (3) is created behind the lens. In the interference region, the P-N beam of a very good quality appears. Unfortunately, this set-up is not convenient for applications because the efficiency of the energy conversion between the input Gaussian beam and the generated P-N beam is very low.

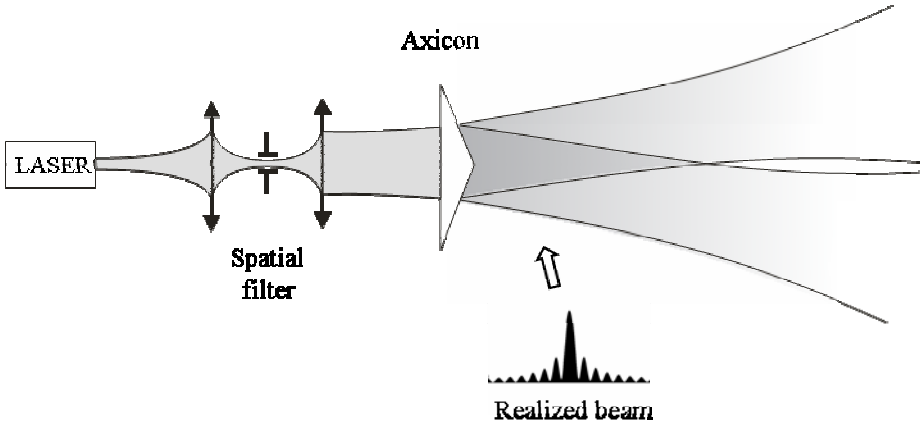

Fig.5 Generation of the pseudo-nondiffracting beam by means of the axicon.

For applications, the optical system utilizing an axicon is more convenient[13]. The generated P-N beam has also a very high quality and represents a good approximation of the zero-order Bessel beam. Furthermore, the energy conversion efficiency is significantly higher in comparison with the Fourier filtration. The radius ρ_0 of the central spot of the created P-N beam depends on the parameters of the axicon and the wavelength of the laser beam and can be approximated by

$$\rho_0 \approx \frac{\lambda}{(n-1)(\pi-\alpha)}, \tag{4}$$

where n and α denote the refractive index and the apex angle of the axicon, respectively. For the P-N beam with the constant spot size, the propagation range can be adjusted by the change of the waist radius of the input collimated laser beam. On the assumption that the aperture of the axicon is larger than the spot size of the input beam, the length of the propagation region can be approximated by

$$L \approx \frac{2\rho_0 w_0}{\lambda}, \tag{5}$$

where w_0 is the waist radius of the Gaussian beam impinging on the axicon. Unlike the Gaussian beam, the propagation range of the beam with the given spot size can be extended if the transverse dimensions of the optics used for generation of the beam are enlarged.

3. ADVANCED EXPERIMENTS ON PSEUDO-NONDIFFRACTING BEAMS

The P-N beams possess some peculiar optical properties not achievable by standard Gaussian beams. In this paper, the potentially applicable properties are reviewed and demonstrated by advanced experiments.

3.1 Dimensional scaling and intensity shaping of the beam

The P-N beam generated by means of the axicon has the spot size unambiguously defined by the wavelength of the used light and by the parameters of the available axicon. If the dimensional scaling of the generated P-N beam is required, it must be additionally transformed by the telescope illustrated in Fig. 6.

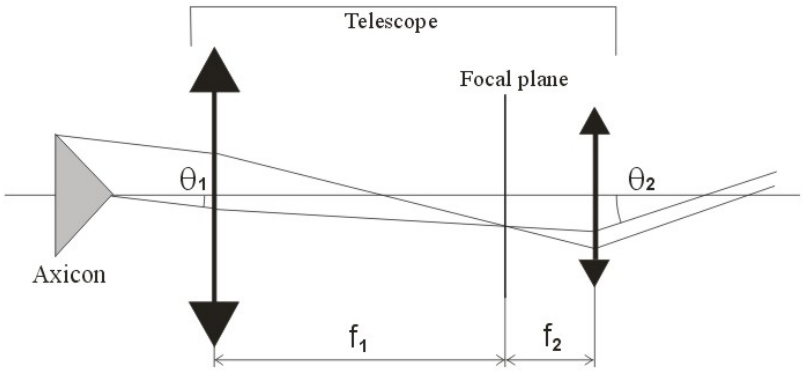

Fig. 6 Optical system for dimensional scaling and intensity shaping of the pseudo-nondiffracting beam.

The telescope is composed of two lenses with focal length f_1 and f_2 so that its angular magnification is given as $\Gamma = -f_1/f_2$. If the beam generated by the axicon has the radius of the central spot ρ_0, the spot radius of the transformed beam behind the telescope is $\rho_0' = \rho_0/\Gamma$. In our experiment, the axicon with the apex angle $\alpha = 179{,}5^\circ$ generating beam with the core radius 0,125 mm was used. By means of the telescope with the angular magnification $\Gamma = 16$, the dimensional rescaling of the beam was realized. The transformed beam appearing behind the telescope had the central spot radius 2 mm. The quality of the beam was very good and it maintained nearly ideal Bessel shape in the propagation region of approximately 100 m. The operation of the telescope can also be explained in terms of the Fourier optics. The front lens of the telescope creates the spatial spectrum of the P-N beam generated by the axicon. It has a shape of the annular ring placed at the front focal plane of the back telescope lens. This lens provides inverse Fourier transform in the way illustrated in Fig. 4. Except of the dimensional scaling of the P-N beam, the shaping of its intensity profile can also be achieved in the set-up illustrated in Fig. 6. It can be realized by azimuthal amplitude or phase modulation of the spatial spectrum at the focal plane. For example, if the spiral phase mask causing the phase change $A = \exp(im\psi)$ is placed there, the zero-order Bessel beam generated by the axicon is transformed and the dark m–th order Bessel beam propagates behind the telescope. By an appropriate design of the modulating phase mask, the splitting of the input Gaussian beam into the array of collinear P-N beams is possible. Furthermore, the separate intensity spots

can be independently shaped into the form approximating predetermined profile. By this way, the variable parallel wireless information channels could be generated by the single transmitter.

3.2 2D positioning of the beam spot

The azimuthal modulation of the spatial spectrum of the P-N beam can also be used for the 2D positioning of the beam spot. The phase change resulting in the required off axis shift of the beam center can be realized by means of the variable wedge prism placed at the focal plane where the spatial spectrum of the P-N beam is localized. A change of the apex angle results in the radial off axis shift of the beam spot [6] (Fig. 7). Rotating the wedge prism round the optical axis, the azimuthal positioning of the beam spot can be achieved. In practice, the variable wedge prism can be realized as the diasporameter.

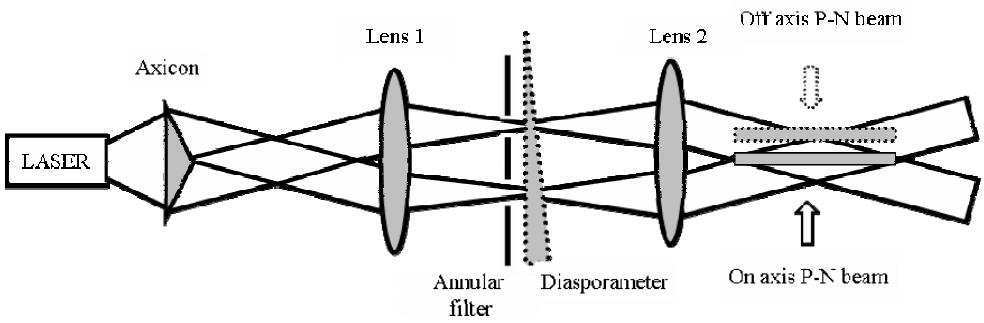

Fig. 7 Optical system enabling navigation of the P-N beam by means of the azimuthal phase modulation of its spatial spectrum.

3.3 Tuning of the beam spatial coherence

In optical wireless communications, a beam robustness against random amplitude and phase distortions is of particular importance [14]. As the P-N beam is created by a conical superposition of plane waves, the small scale obstacles disturb the beam only locally and its intensity profile is restored during subsequent free space propagation (Fig. 8).

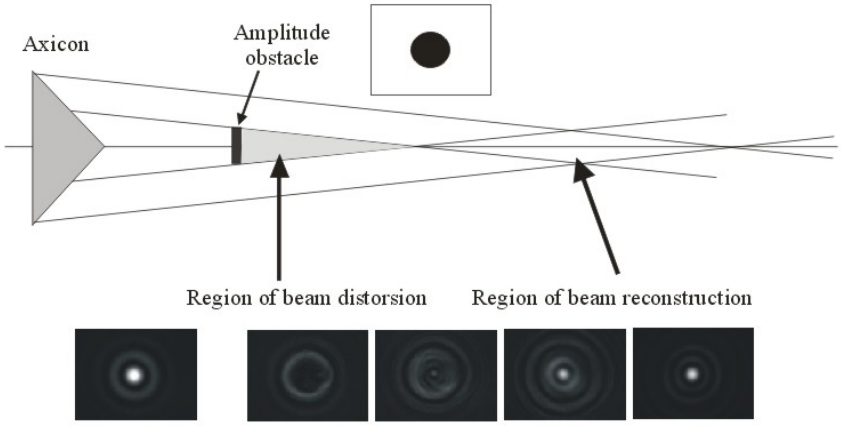

Fig. 8 Experimental demonstration of the robustness of the P-N beam against local amplitude perturbations.

Demonstrated self healing property of the P-N beams is not effective if the random distortions such as atmospheric turbulence strike the whole cross section of the beam[15]. In this case, the decreased spatial coherence of the beam can increase its stability in random fluctuations of the refractive index[16]. By means of the Gauss-Shell model source, the partially coherent P-N beam can be generated. Its spatial coherence can be tuned in a wide range so that both nearly coherent and nearly incoherent beams can be obtained. In the performed experiment, the optical system shown in Fig. 9 was used.

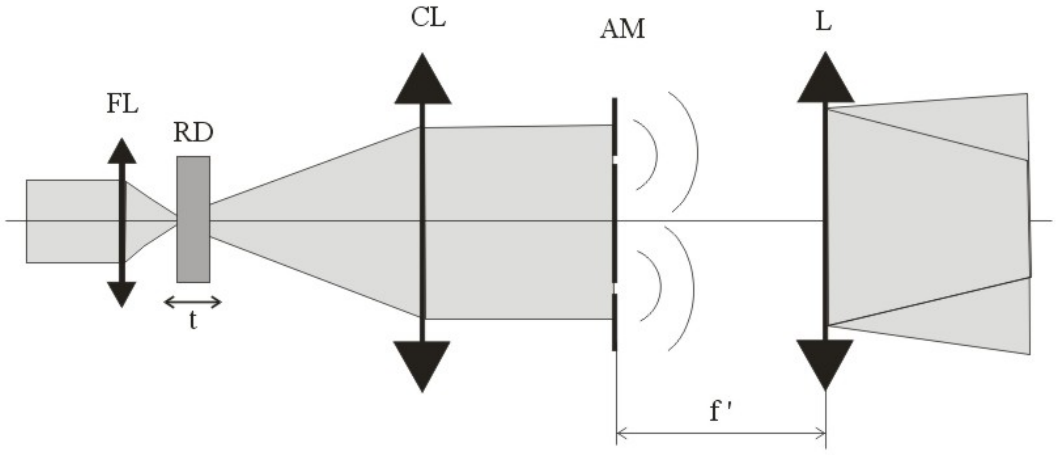

Fig. 9 Generation of the partially coherent pseudo-nondiffracting beam by means of the Gauss-Shell source: FL – focusing lens, RD – rotating diffuser, CL – collimating lens, AM – annular mask, L – lens.

The annular spatial filter placed at the front focal plane of the lens was illuminated by the laser beam transmitted through the rotating diffuser. Changing the size of the beam spot at the diffuser by its longitudinal shift *t*, the spatial coherence of the generated beam can be tuned. In Fig. 10, the intensity profiles of the nearly fully coherent and the partially coherent beams are illustrated. The geometry of the optical system used for generation of the P-N beam was unchanged in both cases, changes of the intensity profile follows from the change of the light spatial coherence. In the case of the partially coherent beam, the adjacent rings are damped and the beam center spot is extended. The degree of the spatial coherence of the light beam illuminating the annular mask was measured in the Young experiment. Two pinholes separated by the distance 1.5 mm were placed into the examined beam and the visibility *V* of the interference pattern measured. The light intensity at the pinholes was balanced, so that the visibility was equal to the degree of spatial coherence at the measured pinholes. For the beam patterns illustrated in Fig. 10 a) and b), the visibility $V = 0,96$ and $V = 0,46$ was obtained.

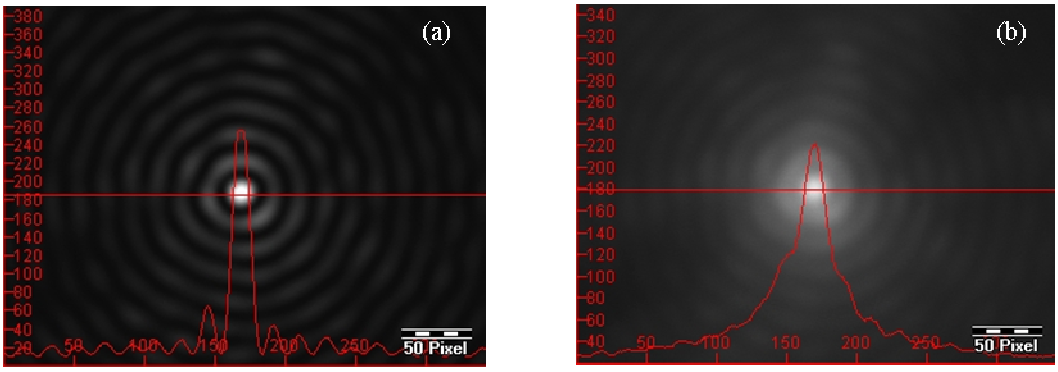

Fig. 10 The pseudo-nondiffracting beams generated by means of the annular spatial filter illuminated by the Gauss-Shell model source enabling tuning of the spatial coherence: (a) nearly fully coherent beam, (b) partially coherent beam.

3.4 Dynamical beam shaping by means of the Spatial Light Modulator

In advanced experiments, the variable P-N beams can be generated by means of the Spatial Light Modulator (SLM) enabling amplitude or phase modulation of the transmitted or reflected laser beam. In our experiments, the amplitude modulator CRL OPTO (1024x768 pixels) and the phase modulator BOULDER (512x512 pixels) are applied. A typical set-up operating with the SLM is illustrated in Fig. 11. The spatially filtered and collimated laser beam impinges on the SLM consisting of an array of pixels created by the electrooptically driven liquid crystals. In a dependence on the SLM design, the amplitude or phase of the input laser beam can be independently changed at the separate pixels. The related amplitude and phase changes are invoked by PC through the so-called computer generated hologram (CGH) sent to the

SLM. The required transformation of the beam is encoded into the CGH adopting principles of holography and special algorithms of diffractive optics. As the CGH causes changes of the refractive index of the liquid crystal pixels resulting in a periodical structure, the input beam splits into several diffraction orders. The power distribution into diffraction orders depends on the design of the CGH. In practice, the blazed gratings are usually applied because most of energy (theoretically 100 %) is directed into the first diffraction order carrying information about the transformed beam. The lens 1 and 2 operate as the 4-f Fourier system enabling elimination of the unwanted diffraction orders. The SLMs are up to date optoelectronic systems with a very wide application potential in various fields of physics and technology. The main advantage of its application is simplicity of operation and a great variability. In contrary to the time-consuming photolitographical methods, the CGH can be produced nearly in real time by means of the SLMs. The refresh rate of the phase SLM BOULDER is approximately 30 Hz but the SLMs with the ferroelectric liquid crystals enable operation with the refresh rate exceeding 1 kHz. A disadvantage of current SLMs is their expensiveness and relative low energetic efficiency usually not exceeding 60 %. In wireless optical communications they can be used for simple realization of multiple spatial channels for transfer of information and for adaptive navigation of the beam disturbed by atmospheric turbulence to the receiver.

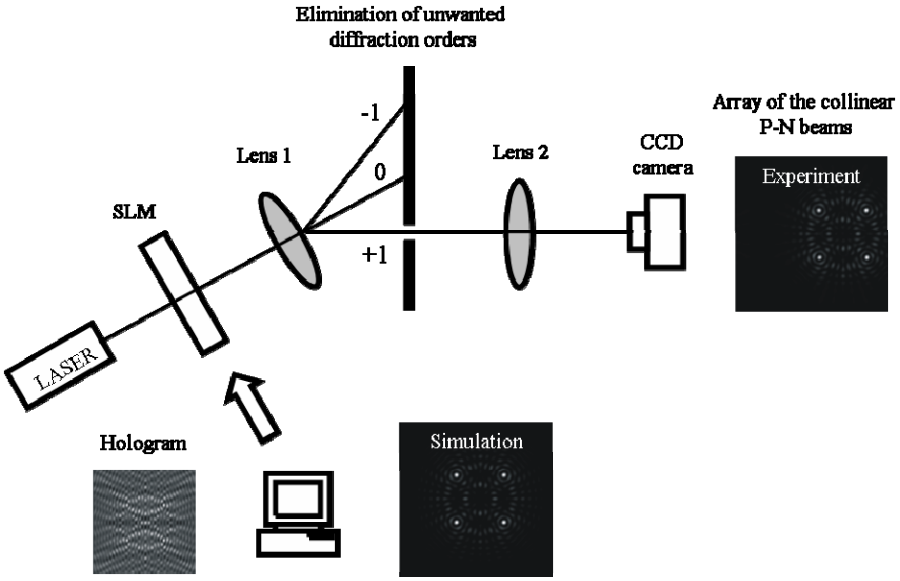

Fig. 11 Optical set-up using the SLM for dynamical shaping of the pseudo-nondiffracting fields.

4. CONCLUSION

In the paper, the physical origin of the nondiffracting propagation of light beams was discussed and the basic properties of the realizable P-N beams interesting for wireless optical communications were reviewed. The basic experiments enabling generation of the P-N beams were presented and their results demonstrated. The advanced experiments enabling generation of the variable P-N fields and arrays of P-N beams were also mentioned. A possibility to perform a dimensional scaling of the P- N beam and its navigation to the receiver was also demonstrated.

ACKNOWLEDGEMENTS

This research has been supported by the Research programs of Brno University of Technology MSM21630513, and by the Grant Agency of the Czech Republic under the contracts No. 102/05/0571, No. 102/05/0732, No. 102/06/1358, No. 102/04/2080 and No. 102/05/732. This research was supported by the projects Center of Modern Optics (LC06007) and Measurement and Information in optics (MSM 6198959213) of the Ministry of Education of the Czech Republic, the project 202/06/0307 of the Czech Grant Agency and by the project FT-TA2/059 of the Ministry of Industry and Trade of the Czech Republic.

REFERENCES

1. C. J. R. Sheppard and T. Wilson, "Gaussian-beam theory of lenses with annular aperture, " *Microwaves Opt. Acoustics* 2, 105 (1978).
2. J. Durnin, "Exact solutions for nondiffracting beams," *J. Opt. Soc. Am. A* 4, 651-654 (1987).
3. V. Bagini, F. Frezza, M. Santarsierro, G. Schettini and G. S. Spagnolo, "Generalized Bessel-Gauss beams," *J. Mod.Opt.* 43, 1155 (1996).
4. Z. Bouchal, "Controlled spatial shaping of nondiffracting patterns and arrays," Opt. Lett. 27, 1376-1378 (2002).
5. Z. Bouchal, "Nondiffracting optical beams: physical properties, experiments, and applications," Czech. J. Phys. 53, 537 (2003).
6. Z. Bouchal, "Physical principle of experiments with pseudo-nondiffracting fields," Czech. J. Phys. 55, 1223-1236 (2005).
7. Z. Bouchal and J. Peřina, "Non-diffracting beams with controlled spatial coherence," *J. Mod. Opt.* 49, 1673-1689 (2002).
8. Z. Bouchal, "Resistance of nondiffracting vortex beam against amplitude and phase perturbations," *Opt. Commun.* 210, 155-164 (2002).
9. J. C. Gutiérrez-Vega and M. A. Bandres, "Helmholtz-Gauss waves," *J. Opt. Soc. Am. A* 22, 289 (2005).
10. W. C. Soares, D. P. Caetano and J. M. Hickman, "Hermite-Bessel beams and the geometrical representation of nondiffracting beams with orbital angular momentum," Opt. Exp. 14, 4577-4582 (2006).
11. M. A. Bandres, J. C. Gutiérrez-Vega and S. Chávez-Cerda, "Parabolic nondiffracting optical wavefields," *Opt. Lett.* 29, 44-46 (2004).
12. J. C. Gutiérrez-Vega, M. D. Iturbe-Castillo and S. Chávez-Cerda, "Alternative formulation for invariant optical fields: Mathieu beams," *Opt. Lett.* 25, 1493-1495 (2000).
13. M. R. Lapointe, "Review of nondiffracting Bessel beam experiments," *Opt. & Laser Technol.* 24, 315-321 (1992).
14. O. Wilfert, Z. Kolka, *Statistical model of free-space optical data link*, Proc. of SPIE – Vol. 5550 Free-Space Laser Communications IV, ed. Jennifer C. Ricklin, David G. Voelz, August 2004, pp. 203-213
15. C. Paterson, "Atmospheric turbulence and orbital angular momentum of single photons for optical communication," *Phys. Rev. Lett.* 94, 153901 (2005).
16. J. C. Ricklin, "Atmospheric turbulence effects on a partially coherent Gaussian beam: implications for free-space laser communication," *J. Opt. Soc. Am. A* 19, 1794-1802 (2002).